HHS Public Access

Author manuscript

J Cardiovasc Electrophysiol. Author manuscript; available in PMC 2018 March 04.

Published in final edited form as:

J Cardiovasc Electrophysiol. 2010 April ; 21(4): 448–454. doi:10.1111/j.1540-8167.2009.01635.x.

Identification of Hemodynamically Unstable Arrhythmias Using Subcutaneous Photoplethysmography

ROBERT G. TURCOTT, M.D., Ph.D.[*] and **TODD J. PAVEK, D.V.M.**[†]

[*]Division of Cardiovascular Medicine, Stanford University School of Medicine, Stanford, California, USA

[†]Center for Animal Resources and Education, Cornell University, Ithaca, New York, USA

Abstract

Introduction—Determination of hemodynamic status is central to arrhythmia management in the inpatient setting. In contrast, therapy decisions in implantable cardioverter defibrillators (ICDs) are based exclusively on the arrhythmia's electrical signature. Hemodynamic sensing in ICDs would allow tailoring of therapy according to perfusion status. Subcutaneous photoplethysmography (PPG) is an attractive technology for this application because it responds to changes in arterial pressure and can be readily incorporated into the housing of implanted devices. This study evaluated the accuracy of PPG in identifying hemodynamically unstable simulated arrhythmias in an animal model.

Methods and Results—Rapid atrial and ventricular pacing was used to simulate arrhythmias in an acute preparation of 7 healthy dogs. Aortic pressure and subcutaneous PPG were simultaneously recorded. Simulated arrhythmias were defined as hemodynamically unstable if aortic pressure decreased by ≥15 mmHg, marginally unstable if pressure decreased by 5–15 mmHg, and hemodynamically stable if pressure either increased or decreased by no more than 5 mmHg. An average of 56 arrhythmias were simulated in each animal. Changes in pressure and PPG output were highly correlated, with correlation coefficient of 0.7–0.9. Subcutaneous PPG identified hemodynamically unstable episodes with a sensitivity of 100% for 6 subjects and 80% for 1 subject. Specificity was more than 90% for 6 subjects and was 50% for 1 subject.

Conclusions—Subcutaneous PPG detects hemodynamically unstable simulated arrhythmias in an acute canine preparation. If successfully validated in humans, this technology may allow ICD therapy to be specifically tailored according to the hemodynamic status of the arrhythmia.

Keywords

photoplethysmography; hemodynamic sensor; arrhythmia; implantable defibrillator

Address for correspondence: Robert Turcott, M.D., Ph.D., Division of Cardiovascular Medicine, Stanford University School of Medicine, Falk CVRC, 300 Pasteur Drive; MC5406, Stanford, CA 94305-5406. Fax: 650-725-1599; turcott@stanford.edu.
St. Jude Medical, Sylmar, California, USA

Background

In contrast to the inpatient setting, where perfusion status is a primary consideration in arrhythmia management,[1] implantable cardioverter defibrillators (ICDs) base therapy decisions exclusively on the electrical activity of the heart. While appropriate therapy is routinely delivered at the extremes of heart rate, accurate rhythm diagnosis for intermediate rates remains challenging despite the advent of dual-chamber devices, which, with the addition of atrial sensing, had been expected to greatly enhance detection accuracy.[2–9] Indeed, recent data suggest that 31% of shock episodes in the postmyocardial infarction, primary prevention population are inappropriate, without a statistically significant difference in the proportion of dual-chamber devices in patients who received versus did not receive inappropriate shocks.[10]

The premise underlying electrogram-based algorithms is that therapy should be delivered for ventricular tachycardia and generally withheld for supraventricular tachycardias.[2] However, this approach is inherently limited by the lack of hemodynamic information. A given rhythm and rate can be hemodynamically stable or unstable, even in the same patient, depending on multiple factors, such as volume status, medications, autonomic tone, and degree of cardiac ischemia. In particular, some episodes of ventricular tachycardia may be hemodynamically stable and well tolerated by the patient, while some episodes of atrial fibrillation may result in symptomatic hypoperfusion. Thus, with electrogram-based algorithms even perfect rhythm diagnosis can lead to inappropriate therapy decisions with respect to hemodynamic status.

Incorporation of hemodynamic sensing functionality into ICDs would allow the device to accelerate therapy for unstable rhythms and either monitor or deliver low-voltage antitachycardia pacing for stable rhythms. The ideal sensor would detect changes in systemic arterial pressure or cardiac output. It would operate from the location of the ICD, thereby avoiding special leads and implant procedures. It would be mechanically stable, be impervious to noise and interference, consume little power, and be transparent to the implanting physician.

Photoplethysmography (PPG) uses light to detect changes in volume of the microvasculature and has been used in a wide variety of clinical applications.[11,12] It is a sensing technology that has many of the features of an ideal hemodynamic sensor. Notably, it responds in a direct proportion to acute changes in systemic blood pressure.[13] The present study quantitatively evaluated the ability of subcutaneous PPG to discriminate hemodynamically unstable arrhythmias from stable arrhythmias that were simulated by rapid pacing in an acute canine preparation.

Methods

Sensor

As previously described,[13] the subcutaneous PPG sensor directs light from an infrared light-emitting diode (LED) to the overlying tissue, with depth of penetration on the order of 1 cm. Much of the light is absorbed or scattered away. The portion that is “reflected” back

(backscattered) to the sensor is detected by a photodiode and converted to an electrical signal. The intensity of the backscattered light is modulated by expansion and contraction of the microvasculature in the overlying tissue. Thus, from a location outside the blood stream, the subcutaneous PPG sensor detects changes in peripheral microvascular volume, which allows changes in arterial pressure to be inferred.[13]

Animal Preparation and Instrumentation

Data were acquired from 7 healthy mongrel dogs of either sex (20–30 kg) in accordance with the Animal Welfare Act. Protocols were approved by the Institutional Animal Care and Use Committee. The animals were fasted overnight, sedated with acepromazine (15 mg SC), induced with thiopental sodium (15–22 mg/kg IV), and maintained with isoflurane (0.8–2.5%) under positive pressure ventilation (tidal volume 10–15 mL/kg, 100% oxygen). Pacing leads were placed in the RA appendage and RV apex via the jugular vein. A high fidelity pressure catheter (Millar Instruments, SPC-340) was placed in the ascending aorta via the femoral artery. The PPG sensor was placed in a subcutaneous pocket in the neck, which afforded a mechanically stable environment. Optical components were oriented deep, toward the underlying muscle layer. Pressure, PPG waveform, and surface ECG were recorded simultaneously.

Pacing Protocol and Data Analysis

Arrhythmias were simulated with bursts of rapid pacing in the RA and RV using 4 different cycle lengths (CLs) delivered to each chamber, specifically, at 250, 293, 353, and 444 ms, which correspond to equally spaced rates between 135 paces/min and 240 paces/min. The order of CLs and pacing chambers were randomized. Rapid pacing was delivered for 10 sec with 20-sec recovery. The change in mean arterial pressure (MAP) was calculated over a 5-sec window immediately preceding and a 10-sec window immediately following the onset of rapid pacing. PPG waveforms were band-pass filtered using cutoff frequencies of 1 and 5 Hz, which attenuated signal components with time scales longer than 1 sec and shorter than 0.2 sec. PPG pulse amplitudes were estimated over the same averaging windows as the MAP. Specifically, each window was divided into 0.5-sec blocks and the pulse amplitude within each block was estimated by calculating the difference δ between the maximum and minimum value of the filtered PPG waveform within the block. The sets of δ were then ordered for each averaging window, and the second ($\delta_{initial}$, 5-sec averaging window) or third (δ_{final},10-sec averaging window) smallest value (i.e., estimated pulse amplitude) was taken as representative of the entire window. The normalized change in PPG pulse amplitude was estimated from these, i.e. $(\delta_{final} - \delta_{initial})/\delta_{initial}$. This approach is sensitive for detecting hemodynamically unstable episodes, avoids the effects of outliers, and is computationally unintensive, a consideration that is important for low-power applications. Correlation between the change in MAP and normalized change in PPG pulse amplitudes was evaluated by scatter plots and the Pearson correlation coefficient.

Sensitivity in detecting hemodynamically unstable episodes and specificity in rejecting hemodynamically stable episodes were calculated. Hemodynamically unstable episodes were defined as those with a reduction in MAP of greater than 15 mmHg, while those for which MAP did not decrease by more than 5 mmHg were defined as stable. Episodes with

decreases in MAP between 5 mmHg and 15 mmHg were defined as marginally unstable, and represent an intermediate region, which, were it a clinical setting, we would view either delivery or withholding of high-voltage therapy as acceptable. Episodes associated with pressure changes in this range were therefore excluded from sensitivity/specificity analysis. The 5- and 15-mmHg pressure boundaries were selected after considering the distribution of pressure changes for the entire ensemble of data, but before testing PPG detection accuracy. Diagnosis was based on the normalized change in PPG pulse amplitude. For each animal, the detection threshold was taken as the largest value that yielded 100% specificity for this classification scheme in first half of the recorded data. Sensitivity and specificity were then calculated using the second half of the data. Postacquisition signal processing and statistical analysis were performed using Matlab (The MathWorks, Natick, MA, USA). Figures were generated using the R statistical computing and graphics package (www.R-project.org).

Results

An example of the changes in aortic pressure (AoP) and PPG waveform induced by rapid RV pacing is shown in Figure 1. There is an abrupt reduction in both MAP and pressure pulse amplitude, shown in the AoP tracing in Panel B. The PPG waveform (C) recapitulates the AoP tracing; the rapid decrease in central arterial mean and pulse pressures is associated with a rapid decrease peripheral arteriolar mean and pulse volumes. Filtering the PPG signal (D) improves noise immunity by blocking the baseline offset and the relatively slow changes in microvascular volume while preserving the pulse amplitude, which decreases with the onset of rapid RV pacing and rebounds above prepacing levels with return to sinus rhythm.

In contrast to RV pacing, with RA pacing (Fig. 2) the ECG shows narrow complexes (A) and the MAP increases (B), likely due to increased cardiac output from the increased heart rate with native ventricular conduction. The aortic pulse pressure, though slightly reduced compared to the baseline rhythm, is still largely preserved. The PPG waveform indicates an increase in average peripheral vascular volume (C), consistent with the increase in MAP. There is a diminution in pulse amplitude as measured by the PPG sensor, which is apparent in both the raw (C) and filtered (D) traces and is consistent with the decrease in aortic pulse pressure seen in panel B.

The distribution of changes in AoP across the ensemble of pacing episodes for all subjects is shown in Figure 3. Changes in MAP ranged from a 37-mmHg decrease to a 15-mmHg increase. The boundaries of the target diagnosis regions are indicated with vertical bars: hemodynamically unstable rhythms are those with decreases in MAP ≥ 15 mmHg and hemodynamically stable rhythms defined as those with MAPs that do not decrease by more than 5 mmHg. Changes in MAP between −15 mmHg and −5 mmHg represent a clinically indeterminate region for which either diagnosis is acceptable.

In Figure 4 the change in MAP is shown plotted against the corresponding normalized change in PPG pulse amplitude for all rapid pacing episodes from one subject. All of the RA (open circles) and many of the RV (filled circles) pacing episodes meet our definition of hemodynamic stability, having changes in MAP that are greater than −5 mmHg. For this animal, this corresponds to a normalized change in PPG greater than approximately −0.8.

Changes in MAP and PPG pulse amplitude are strongly correlated with Pearson correlation coefficient $r = 0.9$, though for the data from this subject the relationship becomes approximately linear only for decreases in MAP.

Figure 5 illustrates the detection analysis using the data presented in Figure 4. The detection threshold was determined from the first half of the recordings, as shown in Panel A. The definitions of hemodynamic stability are shown as horizontal dashed lines at −5 and −15 mmHg. As in Methods, the detection described threshold was taken as the largest normalized change in PPG that provided 100% specificity, i.e., correctly identifying as stable all pacing episodes with MAPs that did not decrease by more than 5 mmHg. For the data of Panel A, varying the detection threshold between −1 and 0 results in the sensitivity and specificity curves shown in Panel B.

The detection threshold derived from the first half of recorded data was then applied to the second half of the data, as shown in Panels C and D of Figure 5. All hemodynamically unstable episodes (change in MAP ≤ −15 mmHg) are to the left of the threshold, resulting in 100% sensitivity. Thirty-five of 36 hemodynamically stable episodes (change in MAP ≥ −5 mmHg) correctly fell to the right of the threshold, resulting in a specificity of 97%. As described under Methods, episodes with changes in MAP between −15 mmHg and −5 mmHg fell in the intermediate region and were excluded from analysis. The effects on sensitivity and specificity of varying the threshold are shown in Panel D using the second half of recorded data. There is a region of thresholds for which both sensitivity and specificity are 100%. Representing detection properties using the receiver–operating characteristic (ROC) would result in a curve with unity area, indicating perfect detection with a retrospectively determined threshold.[14]

Table 1 summarizes the results for all subjects. The change in MAP and normalized PPG pulse amplitude was well correlated across all animals, with r ranging between 0.7 and 0.9. The individualized threshold θ ranged between −0.86 and −0.43. When prospectively applied, the sensitivity was 100% with one exception, which was 80%. In this data set, retrospectively selecting the threshold to give 100% sensitivity while maximizing specificity yields a threshold of $\theta = -0.70$ and a specificity of 91%. Using the prospectively applied thresholds, specificity was greater than 90% for all subjects with a single exception of 50%. In this data set, retrospectively selecting the threshold between −0.99 and −0.64 yields a sensitivity and specificity of 100%.

Discussion

This study demonstrated that a subcutaneously placed extravascular optical sensor could accurately detect hemodynamically unstable simulated arrhythmias in an acute canine model. If validated in humans, it may allow therapy to be specifically targeted to the hemodynamic status of the rhythm. This would represent a fundamentally different approach to ICD-based arrhythmia management and more closely emulate medical practice in an inpatient setting.

Other Approaches to Chronic Hemodynamic Sensing

Basing the therapy decisions of automatic defibrillators on hemodynamic status is not a new concept. Indeed, the first implementation of an automatic defibrillator used RV pressure as a surrogate for systemic hemodynamics.[15] Though a chronic implementation of the sensor initially proved impractical,[16] over the years the approach has been revisited,[17,18] and recently a chronically placed RV pressure sensor has been successfully demonstrated in the context of heart failure monitoring.[19] Other approaches to chronic pressure sensing include placement in the pulmonary artery[20] and left atrium.[21]

Despite the appeal of direct pressure measurement, it either increases the cost and complexity of defibrillation leads while limiting lead/device compatibility or introduces additional intravascular hardware with increased patient risk, both chronically and at device placement. These concerns have motivated the search for a device-based hemodynamic sensor. In addition to PPG, other subcutaneous approaches to identifying hemodynamically unstable arrhythmias include heart sounds[22] and bioimpedance.[23]

The Photoplethsymography Sensor

In addition to avoiding special leads and implant procedures, the subcutaneous PPG requires no moving parts, which greatly enhances the mechanical stability of the sensor. Operating on an optical mechanism allows the sensor to sample the peripheral vasculature at a distance of up to approximately 1 cm from the device. Since light absorption is primarily due to pigments, such as hemoglobin, myglobin, and melanin,[24,25] which are essentially absent in the chronic fibrous encapsulation, the capsule is expected to be largely transparent to the wavelengths of interest. This hypothesis has been supported by both a chronic animal study, which demonstrated stability of the PPG signal over 4–9 months,[26] and an acute human study, in which PPG signals were readily detected by a subcutaneous sensor placed in a mature ICD pocket.[27] Modest evolution in signal amplitudes that does occur with chronic fibrosis or other factors, such as changes in vascular density, should not influence hemodynamic sensing since, by design, the analysis focuses on changes in pulse amplitude that occur over very short time scales.

Motion artifact is a challenge for all mechanical sensors. With PPG the signal amplitude is on the order of a few percent of the total detected (backscattered) light.[13] Effects that influence the baseline backscattered light (e.g., changes in tissue compression, tissue sheer, and venous blood volume induced by change in posture) have the potential to dominate the signal associated with the change in arteriolar volume. We minimize this potential by narrow-band filtering, which eliminates the effect of baseline shift by focusing only on the change in pulse amplitude. This approach also reduces the effect of changes in ambient light on sensor performance. In addition, the device housing provides significant shielding for sensors. Other techniques for minimizing the effect of motion include differential sensors with common mode rejection, adaptive filters, and, perhaps most importantly, confirmation of signal quality before incorporating the sensor output into therapy decisions. Potential solutions to other PPG-specific technical challenges, such as power consumption, have been discussed previously.[13]

Study Protocol

This initial proof-of-concept study used an acute preparation of healthy dogs in which ventricular and supraventricular arrhythmias were simulated with rapid pacing. The hemodynamic consequences of the simulated arrhythmias were as expected, with an acute fall in blood pressure induced by high-rate ventricular pacing and maintenance of pressure with atrial pacing. PPG allowed accurate detection in this limited initial study. We anticipate improvement in accuracy and an increased ability to accommodate the nuances seen in spontaneous arrhythmias as detection algorithms are further developed and refined. Conducting a similar protocol during ICD implant, electrophysiology study, or arrhythmia ablation, would allow proof-of-concept testing in humans and begin the process of mapping changes in MAP to PPG amplitudes in human subjects.

Clinical Implications

Currently, ICD analysis is based exclusively on the electrical signature of the rhythm. Despite the introduction of dual-chamber devices, the diagnostic accuracy remains limited.[2–10,28] Importantly, even with perfect arrhythmia diagnosis, electrogram analysis does not reveal information about the underlying hemodynamic status of the patient. Incorporating hemodynamic information into the arrhythmia detection algorithm of an ICD would allow the device to more closely emulate arrhythmia management in the inpatient setting, where therapy decisions depend critically on the assessment of perfusion status.[1]

In the present study, the MAP axis was partitioned into 3 regions that reflect 3 different treatment goals: unstable arrhythmias requiring high-voltage therapy, stable arrhythmias for which high-voltage therapy is not immediately necessary, and arrhythmias of marginal stability, for which either delivering or withholding high-voltage therapy would be reasonable. Partitioning in this way imposed a 10-mmHg precision on the detection characteristic; we are effectively asking the sensor to detect hemodynamically unstable rhythms, with a precision of 10 mmHg. The tripartite definition avoids the artificial dichotomy of a binary partition in which a small change in pressure could nominally have a potentially dramatic change in the desired therapy. A similar approach is used in other clinical settings in which a continuous parameter is dichotomized into “normal” and “pathologic” regions with an interposed intermediate region, e.g., “prehypertension”[29] and “impaired fasting glucose.”[30]

Other potential applications of PPG include automatic optimization of atrioventricular and interventricular pacing intervals,[31] respiration monitoring,[32] monitoring of arterial oxygen saturation for chronic disease management, and automatic determination of upper and lower rate cutoff in rate-responsive pacemakers.

Limitations

In this initial proof-of-concept study, arrhythmias were simulated by rapid pacing in an acute preparation using a small number of healthy animals. Potential technical challenges discussed above, such as encapsulation and motion artifact, were not addressed. The simulated arrhythmias do not reproduce important details of spontaneously occurring

rhythms, such as an initial pressure decay followed by recovery seen in some stable arrhythmias and the variability in RR intervals seen in atrial fibrillation. Other significant differences between the present study and sensor use in the target population include the location of the device, degree of adipose tissue and vascular density, vasoactive medications, cardiac output and vascular resistance, autonomic dysfunction, and atherosclerosis. While the general relationship between acute changes in MAP and PPG observed here can be expected to hold in humans, studies using chronically implanted sensors in ambulatory ICD recipients with data collected during spontaneously occurring rhythms will be necessary to validate this approach to arrhythmia discrimination based on hemodynamic stability.

Conclusions

This proof-of-concept study demonstrated the ability of an extravascular, subcutaneously placed optical sensor to identify hemodynamically unstable simulated arrhythmias in healthy dogs. Good detection sensitivity and specificity were achieved with a detection precision of 10 mmHg. Hemodynamic sensing using subcutaneous PPG may allow specific tailoring of antiarrhythmia therapy based on the hemodynamic status of the rhythm.

Acknowledgments

We wish to thank Drs. Euan A. Ashley and Paul J. Wang for their critical review and feedback; Tim Fayram and the Sunnyvale research group for numerous insightful and thought-provoking discussions; and John Chu for his expertise and assistance in constructing and preparing the sensor and data-acquisition circuit.

Dr. Turcott is supported by National Library of Medicine Biomedical Informatics Training Grant LM 07033.

This work was sponsored by St. Jude Medical and was conducted while the authors were full-time employees of the company. Neither author presently has a professional relationship with or financial interest in the company or in the intellectual property related to this subject. The authors have had complete control over the data and preparation of the manuscript, and have not received payment for its preparation.

References

1. 2005 American Heart Association guidelines for cardiopulmonary resuscitation and emergency cardiovascular care. Circulation. 2005; 112:IV1–IV203. [PubMed: 16314375]
2. Berger RD, Lerew DR, Smith JM, Pulling C, Gold MR. The Rhythm ID Going Head to Head Trial (RIGHT): Design of a randomized trial comparing competitive rhythm discrimination algorithms in implantable cardioverter defibrillators. J Cardiovasc Electrophysiol. 2006; 17:749–753. [PubMed: 16836672]
3. Boriani G, Biffi M, Dall'Acqua A, Martignani C, Frabetti L, Zannoli R, Branzi A. Rhythm discrimination by rate branch and QRS morphology in dual chamber implantable cardioverter defibrillators. Pacing Clin Electrophysiol. 2003; 26:466–470. [PubMed: 12687869]
4. Hintringer F, Deibl M, Berger T, Pachinger O, Roithinger FX. Comparison of the specificity of implantable dual chamber defibrillator detection algorithms. Pacing Clin Electrophysiol. 2004; 27:976–982. [PubMed: 15271019]
5. Theuns DA, Klootwijk AP, Goedhart DM, Jordaens LJ. Prevention of inappropriate therapy in implantable cardioverter-defibrillators: Results of a prospective, randomized study of tachyarrhythmia detection algorithms. J Am Coll Cardiol. 2004; 44:2362–2367. [PubMed: 15607399]
6. Al-Ahmad A, Tsiperfal A, Hsia HH, Wang PJ. Inappropriate shock: A failure of SVT discriminators in a dual chamber ICD? Pacing Clin Electrophysiol. 2006; 29:1413–1415. [PubMed: 17201851]
7. Lee KL, Lau CP. Inappropriate defibrillator therapies: Are dual chamber devices providing a remedy? J Cardiovasc Electrophysiol. 2001; 12:143–144. [PubMed: 11232609]

8. Deisenhofer I, Kolb C, Ndrepepa G, Schreieck J, Karch M, Schmieder S, Zrenner B, Schmitt C. Do current dual chamber cardioverter defibrillators have advantages over conventional single chamber cardioverter defibrillators in reducing inappropriate therapies? A randomized, prospective study. J Cardiovasc Electrophysiol. 2001; 12:134–142. [PubMed: 11232608]
9. Theuns DA, Rivero-Ayerza M, Boersma E, Jordaens L. Prevention of inappropriate therapy in implantable defibrillators: A meta-analysis of clinical trials comparing single-chamber and dual-chamber arrhythmia discrimination algorithms. Int J Cardiol. 2008; 125:352–357. [PubMed: 17445918]
10. Daubert JP, Zareba W, Cannom DS, McNitt S, Rosero SZ, Wang P, Schuger C, Steinberg JS, Higgins SL, Wilber DJ, Klein H, Andrews ML, Hall WJ, Moss AJ. Inappropriate implantable cardioverter-defibrillator shocks in MADIT II: Frequency, mechanisms, predictors, and survival impact. J Am Coll Cardiol. 2008; 51:1357–1365. [PubMed: 18387436]
11. Allen J. Photoplethysmography and its application in clinical physiological measurement. Physiol Meas. 2007; 28:R1–R39. [PubMed: 17322588]
12. Shelley KH. Photoplethysmography: Beyond the calculation of arterial oxygen saturation and heart rate. Anesth Analg. 2007; 105:S31–S36. Tables of contents. [PubMed: 18048895]
13. Turcott RG, Pavek TJ. Hemodynamic sensing using subcutaneous photoplethysmography. Am J Physiol Heart Circ Physiol. 2008; 295:H2560–H2572. [PubMed: 18849335]
14. Metz CE. Basic principles of ROC analysis. Semin Nucl Med. 1978; 8:283–298. [PubMed: 112681]
15. Mirowski M, Mower MM, Staewen WS, Tabatznik B, Mendeloff AI. Standby automatic defibrillator. An approach to prevention of sudden coronary death. Arch Intern Med. 1970; 126:158–161. [PubMed: 5425512]
16. Kastor JA. Michel Mirowski and the automatic implantable defibrillator. Am J Cardiol. 1989; 63:1121–1126. [PubMed: 2650518]
17. Ellenbogen KA, Wood MA, Kapadia K, Lu B, Valenta H. Short-term reproducibility over time of right ventricular pulse pressure as a potential hemodynamic sensor for ventricular tachyarrhythmias. Pacing Clin Electrophysiol. 1992; 15:971–974. [PubMed: 1378606]
18. Cohen TJ, Liem LB. Biosensor applications to antitachycardia devices. Pacing Clin Electrophysiol. 1991; 14:322–328. [PubMed: 1706846]
19. Bourge RC, Abraham WT, Adamson PB, Aaron MF, Aranda JM Jr, Magalski A, Zile MR, Smith AL, Smart FW, O'Shaughnessy MA, Jessup ML, Sparks B, Naftel DL, Stevenson LW. Randomized controlled trial of an implantable continuous hemodynamic monitor in patients with advanced heart failure: the COMPASS-HF study. J Am Coll Cardiol. 2008; 51:1073–1079. [PubMed: 18342224]
20. Verdejo HE, Castro PF, Concepcion R, Ferrada MA, Alfaro MA, Alcaino ME, Deck CC, Bourge RC. Comparison of a radiofrequency-based wireless pressure sensor to swanganz catheter and echocardiography for ambulatory assessment of pulmonary artery pressure in heart failure. J Am Coll Cardiol. 2007; 50:2375–2382. [PubMed: 18154961]
21. Walton AS, Krum H. The Heartpod implantable heart failure therapy system. Heart Lung Circ. 2005; 14(Suppl 2):S31–S33. [PubMed: 16352285]
22. Kobza R, Roos M, Toggweiler S, Zuber M, Erne P. Recorded heart sounds for identification of ventricular tachycardia. Resuscitation. 2008; 79:265–272. [PubMed: 18656299]
23. Venugopal D, Patterson R, Jhanjee R, McKnite S, Lurie KG, Belalcazar A, Benditt DG. Subcutaneous bioimpedance recording: assessment of a method for hemodynamic monitoring by implanted devices. J Cardiovasc Electrophysiol. 2009; 20:76–81. [PubMed: 18691232]
24. Sinex JE. Pulse oximetry: Principles and limitations. Am J Emerg Med. 1999; 17:59–67. [PubMed: 9928703]
25. Zijlstra WG, Buursma A, Meeuwsen-van der Roest WP. Absorption spectra of human fetal and adult oxyhemoglobin, de-oxyhemoglobin, carboxyhemoglobin, and methemoglobin. Clin Chem. 1991; 37:1633–1638. [PubMed: 1716537]
26. Nabutovsky Y, Wright G, Pavek TJ, Turcott RG. Chronic performance of a subcutaneous photoplethysmography sensor (abstract). Heart Rhythm. 2004; 1:S151.

27. Weiss EH, Weaver L, Fang M, Tamhidi L, Kang P, Tomassoni G, Gallagher P, Hesselson A, Sharma A, O'Neill G, Ackerman S, Turk K, Rodrigues D. Evaluation of a subcutaneous photoplethysmography sensor in mature ICD pockets (abstract). Heart Rhythm. 2006:P3–P84.

28. Poole JE, Johnson GW, Hellkamp AS, Anderson J, Callans DJ, Raitt MH, Reddy RK, Marchlinski FE, Yee R, Guarnieri T, Talajic M, Wilber DJ, Fishbein DP, Packer DL, Mark DB, Lee KL, Bardy GH. Prognostic importance of defibrillator shocks in patients with heart failure. N Engl J Med. 2008; 359:1009–1017. [PubMed: 18768944]

29. Chobanian AV, Bakris GL, Black HR, Cushman WC, Green LA, Izzo JL Jr, Jones DW, Materson BJ, Oparil S, Wright JT Jr, Roccella EJ. The seventh report of the joint national committee on prevention, detection, evaluation, and treatment of high blood pressure: The JNC 7 report. JAMA. 2003; 289:2560–2572. [PubMed: 12748199]

30. Report of the expert committee on the diagnosis and classification of diabetes mellitus. Diabetes Care. 1997; 20:1183–1197. [PubMed: 9203460]

31. Turcott RG, Pavek TJ. Pacing interval optimization using photoplethysmography (abstract). J Card Fail. 2004; 10:S73.

32. Turcott RG, Pavek TJ. Detection of hypopnea using subcutaneous photoplethysmography (abstract). J Card Fail. 2005; 11:S113.

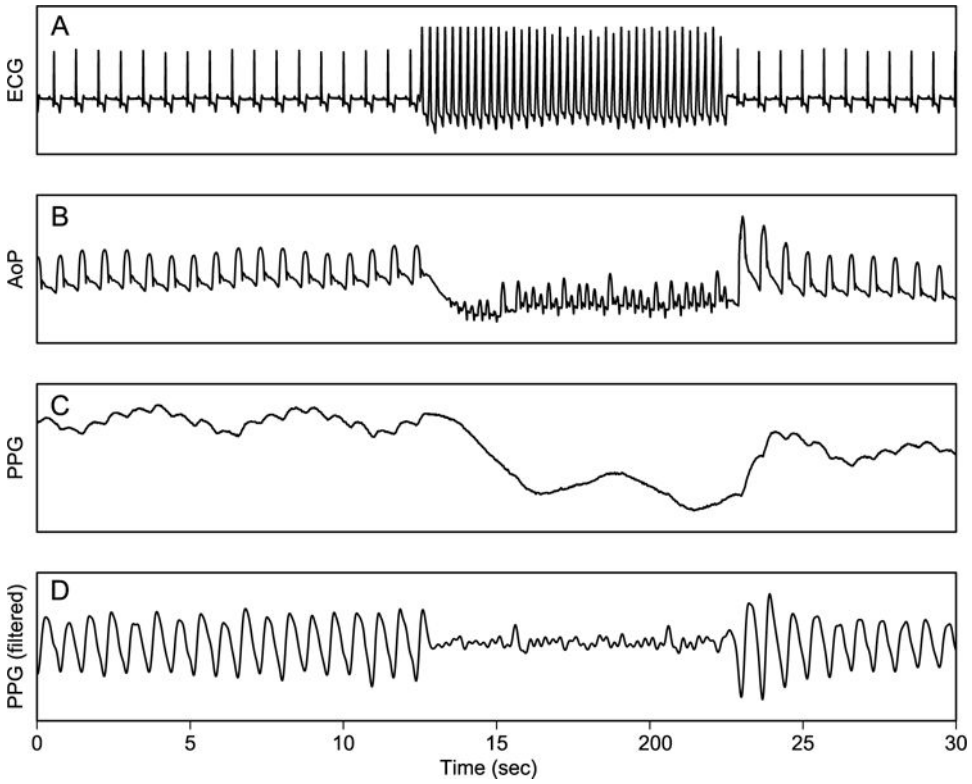

Figure 1.

Simulated ventricular arrhythmia. Ten sec of rapid RV pacing with a cycle length of 250 ms is initiated at approximately 13 sec. (A) ECG, showing normal sinus rhythm prior to and after the burst of rapid pacing. (B) Aortic pressure (AoP). There is an acute decrease in both mean and pulse pressures with the onset of rapid pacing. (C) Subcutaneous photoplethysmography (PPG). The change in subcutaneous arteriolar volume as measured by PPG recapitulates the change in central mean and pulse pressures. (D) Filtering the PPG waveform preserves the pulse amplitude while eliminating changes that occur over shorter and longer time scales. The decrease in PPG pulse amplitude with rapid pacing is readily apparent.

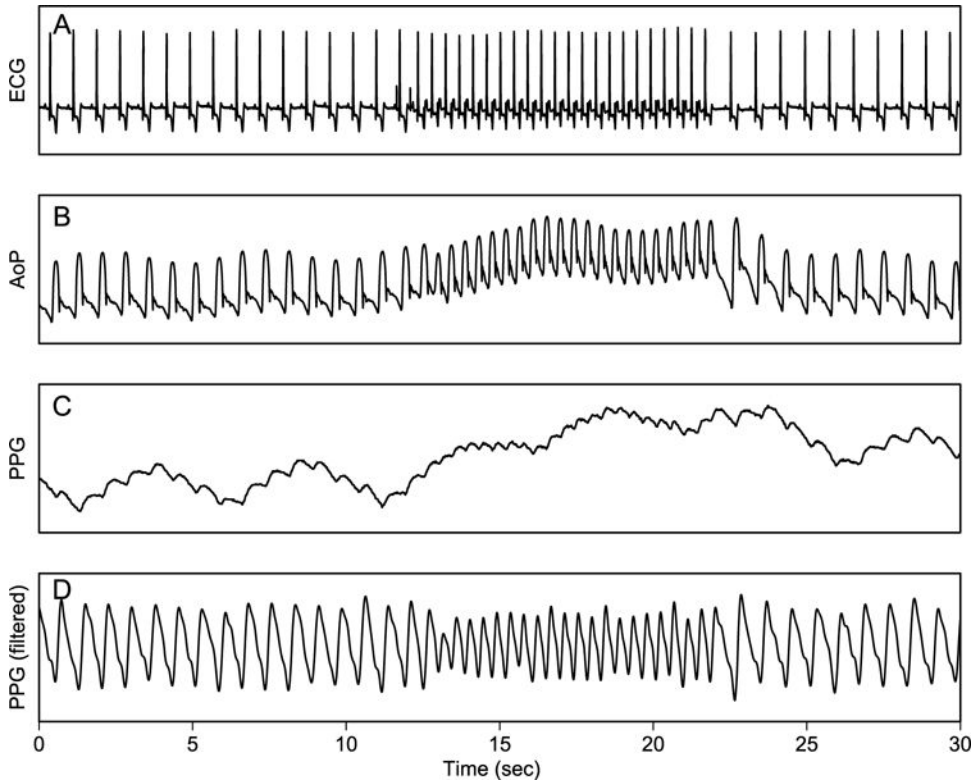

Figure 2.

Simulated atrial arrhythmia. Ten sec of rapid RA pacing with 440-ms cycle length is initiated at approximately 12 sec. Panels are analogous to Figure 1. There is an increase in mean aortic pressure (AoP) with the onset of pacing. Aortic pulse pressure is somewhat diminished relative to sinus rhythm, as is the peripheral arteriolar pulse volume as measured by photoplethysmography (PPG).

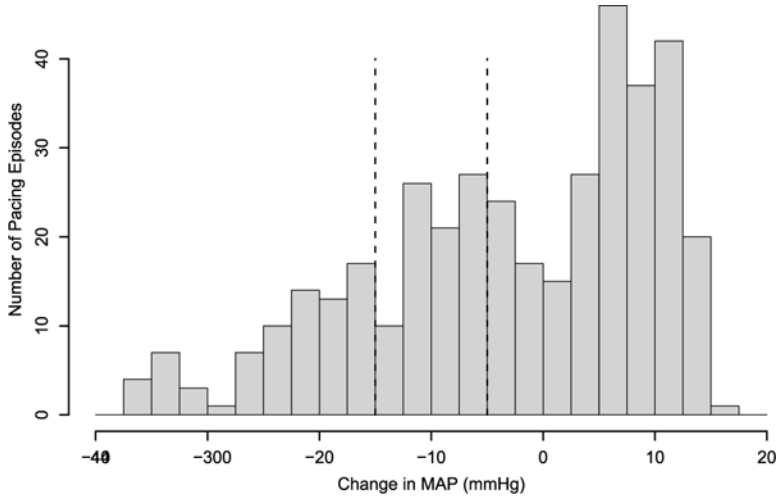

Figure 3.

Change in average aortic pressure with rapid pacing. The histogram includes all recorded episodes for all subjects. The simulated arrhythmias were defined to be unstable if the mean arterial pressure (MAP) decreased by 15 mmHg or more, and stable if the MAP did not decrease by more than 5 mmHg.

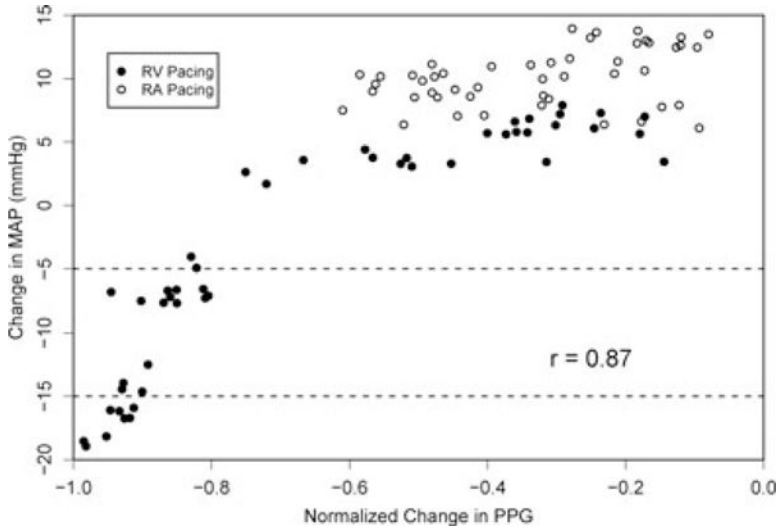

Figure 4.

Pacing-induced changes in pressure and volume. The change in mean arterial pressure (MAP) and normalized photoplethysmography (PPG) pulse amplitude are shown for each rapid pacing episode in one subject. RA pacing (open circles) resulted in an acute increase in MAP, while RV pacing (filled circles) had a variable effect, depending on the pacing rate. While the 2 measures are generally well correlated, with r = 0.9, in this subject the relationship is clearly nonlinear, except perhaps for arrhythmias that induce a decrease in MAP.

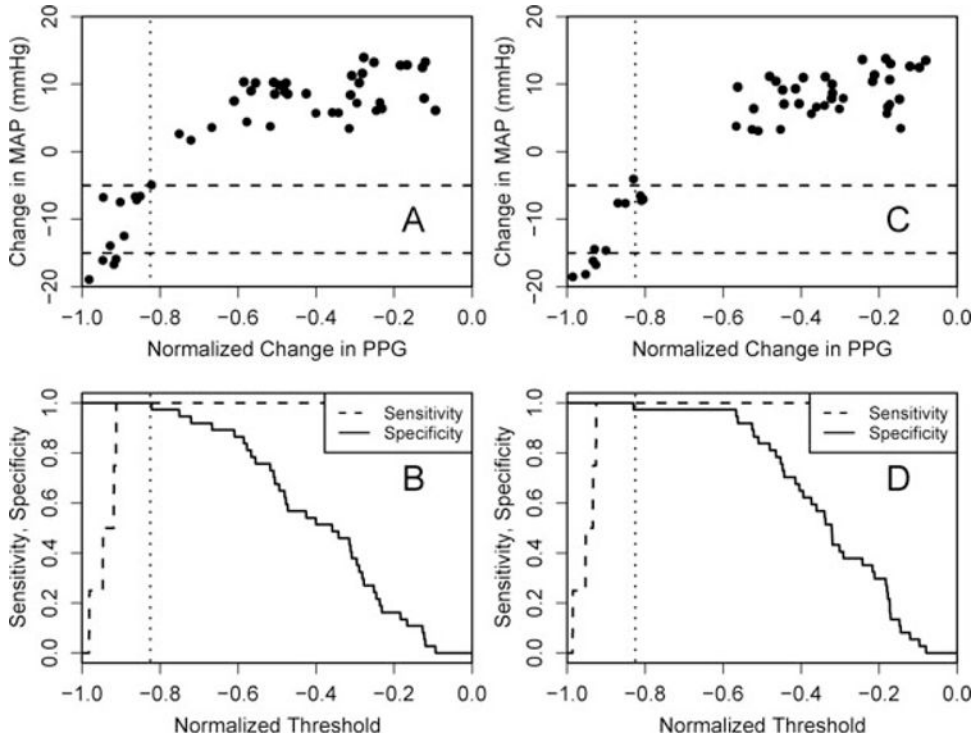

Figure 5.

Detection threshold and accuracy. (A) Using the first half of the data as shown in Figure 4, the detection threshold θ is set to the largest value of the change in normalized PPG pulse amplitude that yielded 100% specificity (vertical dotted line). The definitions of hemodynamic stability are illustrated using horizontal dashed lines at −5 and −15 mmHg. (B) Sensitivity and specificity curves that result using the data of Panel A as the threshold are varied between −1 and 0. (C) Application of the threshold determined in Panel A to the second half of recorded data. One of 36 stable episodes was incorrectly classified as unstable. (D) Sensitivity and specificity curves for the second half of recorded data. The predetermined threshold is shown as a vertical dotted line.

TABLE 1

Detection Characteristics

Subject	N	*r*	Sensitivity	Specificity	*θ*
1	24	0.88	1.00	1.00	−0.43
2	23	0.83	1.00	0.50	−0.47
3	64	0.70	1.00	1.00	−0.63
4	48	0.87	1.00	0.92	−0.48
5	96	0.87	1.00	0.97	−0.82
6	46	0.70	0.80	1.00	−0.86
7	88	0.86	1.00	1.00	−0.61

N = number of rapid pacing episodes; r = Pearson's correlation coefficient; θ detection threshold.